

WHOI-84-44

**SUMMER STUDY PROGRAM
in
Geophysical Fluid Dynamics
Woods Hole Oceanographic Institution**

DYNAMIC DIFFERENTIATION

by

Willem V. R. Malkus, Director
and
Florence K. Mellor, Editor

Woods Hole Oceanographic Institution
Woods Hole, Massachusetts 02543

November 1984

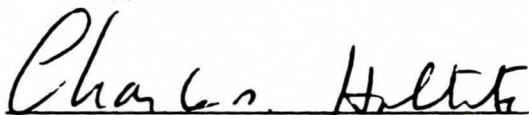
Technical Report

*Prepared for the Office of Naval Research under contract
N00014-82-G-0079 and the National Science Foundation under Grant
MCS-82-000450. Partial support acknowledged from the Center for Analysis
of Marine Systems (CAMS) at the Woods Hole Oceanographic Institution.
CAMS is supported by The Exxon Foundation, Mobil Foundation, Inc., The
Ambrose Monell Foundation, The R. R. Mellon Family Foundation, the Atlantic
Richfield Foundation, and by an anonymous donor.*

*Reproduction in whole or in part is permitted for any purpose of the United
States Government. This report should be cited as Woods Hole Oceanog. Inst. Tech.
Rept. WHOI-84-44.*

Approved for public release; distribution unlimited.

Approved for Distribution:



Charles D. Hollister
Dean of Graduate Studies

PARTICULATE DISPERSAL IN A TIME-DEPENDENT FLOW
Leonard A. Smith

1. INTRODUCTION

Questions concerning the suspension and fall out of negatively buoyant particles are of central importance in several fields of current research. They arise in a wide range of phenomena including precipitation formation and the lifetime of volcanic aerosols in the atmosphere, suspension of plankton in the sea and geophysical processes such as the suspension of growing crystals in a convecting magma chamber. As an initial step toward understanding such phenomena, we examine the motion of particles in a simple laminar flow which is periodic in time. Stommel (1949) developed the theory for the case of steady rolls. Experimental investigations of a similar steady flow field have been performed by Tooby et. al. (1977). Aref (1984) has modeled the stirring of a tank of fluid by point vortices. This paper outlines the analytic treatment of the time-dependent case to third order and presents the results of numerical experiments over a wide range of conditions. In addition to regions of retention and simple fallout, regions of chaotic particle motions, including some in which the particle slowly migrates downward through a series of cells, are observed. Initial observations concerning the stabilization of particles which would fall out of the steady mean flow are discussed.

The dynamical system representing particle motion is of interest in its own right. It is a two-dimensional Hamiltonian system, periodic in both space and time, so the phase space of the system is three-dimensional and of finite volume, and therefore may be easily visualized. Two-dimensional Poincare sections of phase space reveal regions in which particle motion is described by either a simple torus, a twisted torus (islands), the breakup of islands into chaotic regions, sheets which act as barriers to particle motion and the breakdown of these sheets into islands and then chaotic regions. Which behavior a particle will display depends on its initial position and the strength and frequency of the oscillations. Hamiltonian chaos is most commonly observed in three-dimensional systems. In this system, the role of the third degree of freedom is played by the explicit time dependence of the Hamiltonian.

2. STEADY BACKGROUND FLOW

The suspension of negatively buoyant particles in horizontal fluid rolls is easily observed in the laboratory. The standard apparatus consists of a cylindrical tank filled with a high viscosity fluid and mounted with its axis horizontal. As the cylinder is rotated about its axis, the fluid quickly (~ 10 seconds) reaches solid body rotation. Small spheres placed in the ascending flow are observed to follow nearly circular orbits about the particle stagnation point, where the fluid velocity is equal to the negative of the particle settling velocity. In addition to the negatively buoyant particles, several small, almost spherical air bubbles (positively buoyant) were observed to execute similar motion in the descending fluid on the opposite side of the tank. A detailed investigation of this system has been performed by Tooby, Wick and Isaacs (1977), using a tank 15 cm. in diameter, with test particles of radius between 0.8 mm. and 3.0 mm. and rotational periods in the range 5.0 to 40.0 seconds. They find that particle orbits generally have periods slightly greater than that of the fluid. On longer time scales the

orbits evolve, the radius changing by a factor of two in 30 to 100 fluid oscillations. The density and diameter of the test particle determine whether its orbit grows or contracts. This instability is due to inertial effects and the influences of the walls on finite diameter test particles. Particle-particle interactions are also observed to produce large perturbations in particle motions (Whitehead, private communication). In the cases of precipitation formation and magma crystal growth, the properties of a single particle change influencing the particle's motion, which in turn feeds back upon the particle's growth. None of these complicating effects are considered here.

The effect of steady convective rolls on the motion of a small, slowly sinking body was first investigated by Stommel (1949). This work was stimulated by the observation that the yield of the plankton tows taken along the direction of the wind, and therefore parallel to the axis of wind-induced fluid rolls, were much more variable than those from tows taken perpendicular to the wind. Stommel considered a particle slowly sinking through fluid rolls with a stream function.

$$\Psi_F(x,y) = A \sin x \sin y \quad (2.1)$$

where the subscript F denotes the fluid, x is measured in the horizontal direction and y in the vertical. The streamlines of this flow are shown in figure 1. The velocity of the particle is that of the fluid plus a settling velocity, v_s , in the negative y direction. Specifically,

$$\begin{aligned} \frac{dx}{dt} = \dot{x} &= \frac{\partial \Psi_F}{\partial y} = A \sin x \cos y \\ \frac{dy}{dt} = \dot{y} &= -\frac{\partial \Psi_F}{\partial x} - v_s = -A \cos x \sin y - v_s \end{aligned} \quad (2.2)$$

Thus the particle motion has a stream function

$$\Psi_P(x,y) = A \sin x \sin y + v_s x \quad (2.3)$$

Particle trajectories may be classified by the ratio of the settling velocity to a measure of the maximum fluid velocity:

$$s = \frac{v_s}{A} \quad (2.4)$$

In the case $s = 0$ the particles are neutrally buoyant and follow the streamlines of the fluid. For $s > 1$ (or $s < -1$), all particles fall (rise) through the cells, horizontally displaced away from the region of maximum fluid up-flow. This displacement results from sinking (rising) particles having minimum vertical velocity in regions of maximum upward (downward) fluid velocity. This increases their residence time in the area, and hence their horizontal displacement from the background flow.

For an intermediate value, $-1 < s < 1$ there exists a region of retention in which particles will execute closed orbits, and therefore, remain suspended in the cell. Streamlines of particle motion for several values of s are shown in figure 2. The boundary of the region of retention is delineated by the largest closed orbit within the cell. Along this boundary the particle stream function has the same value it takes along the cell border. This may be seen in figure 2. In the steady case, this is the orbit of a particle which rises (sinks) infinitesimally close to the upward (downward) flow at the

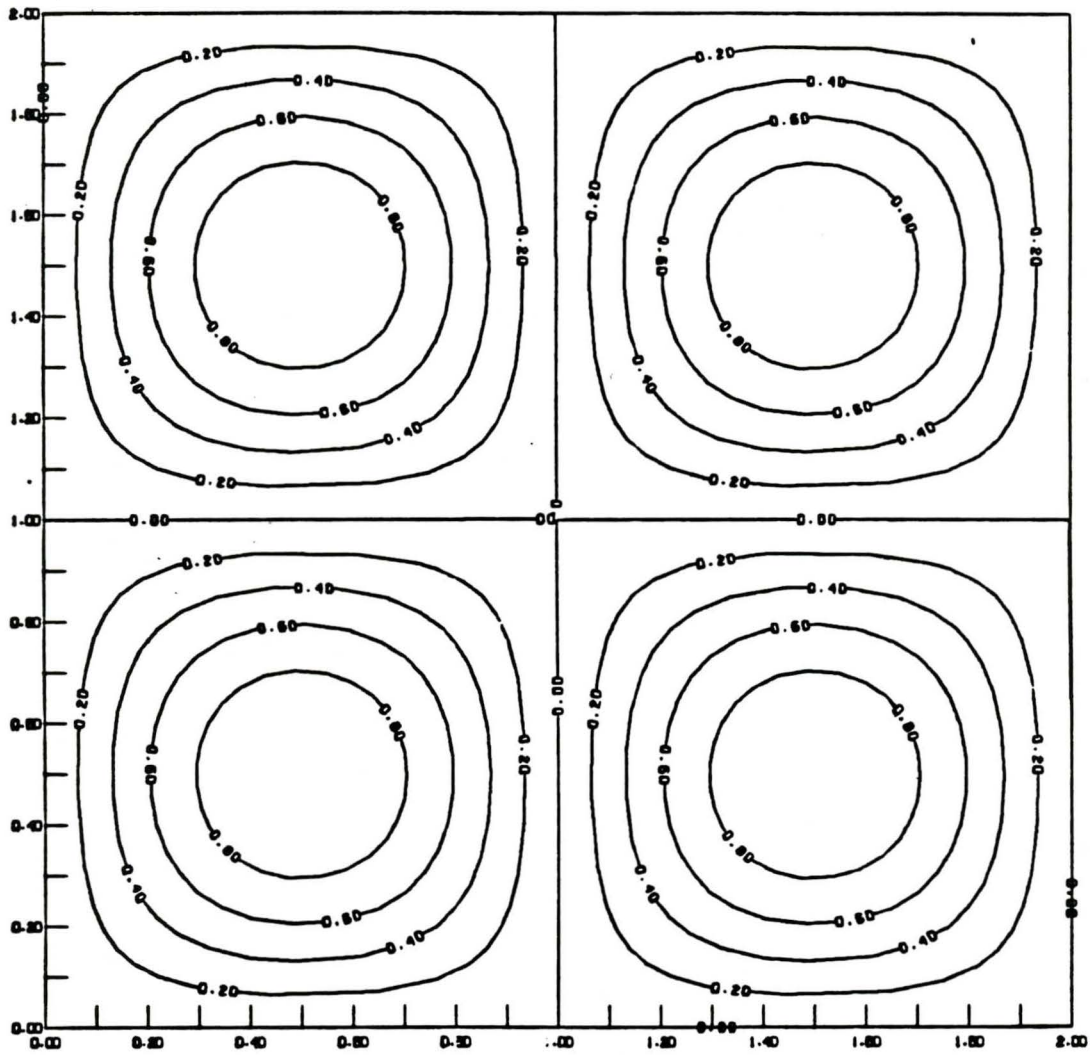


Figure 1

Streamlines of the background flow field described by equation 2.1 .

$s = 0.25$

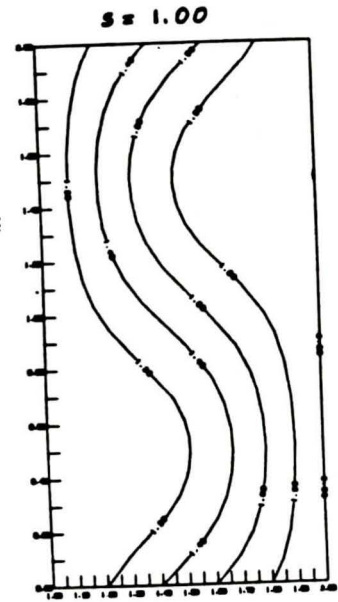
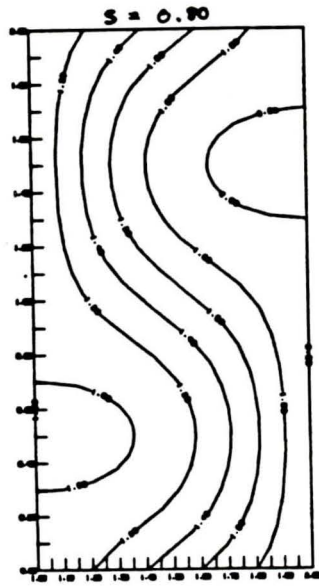
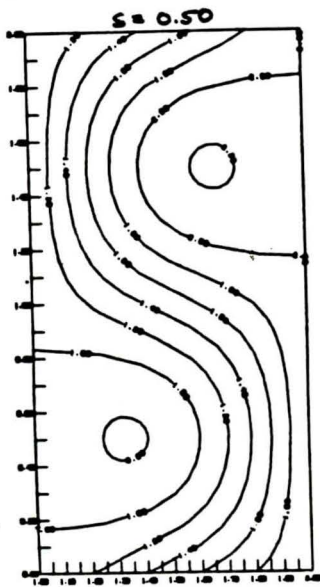
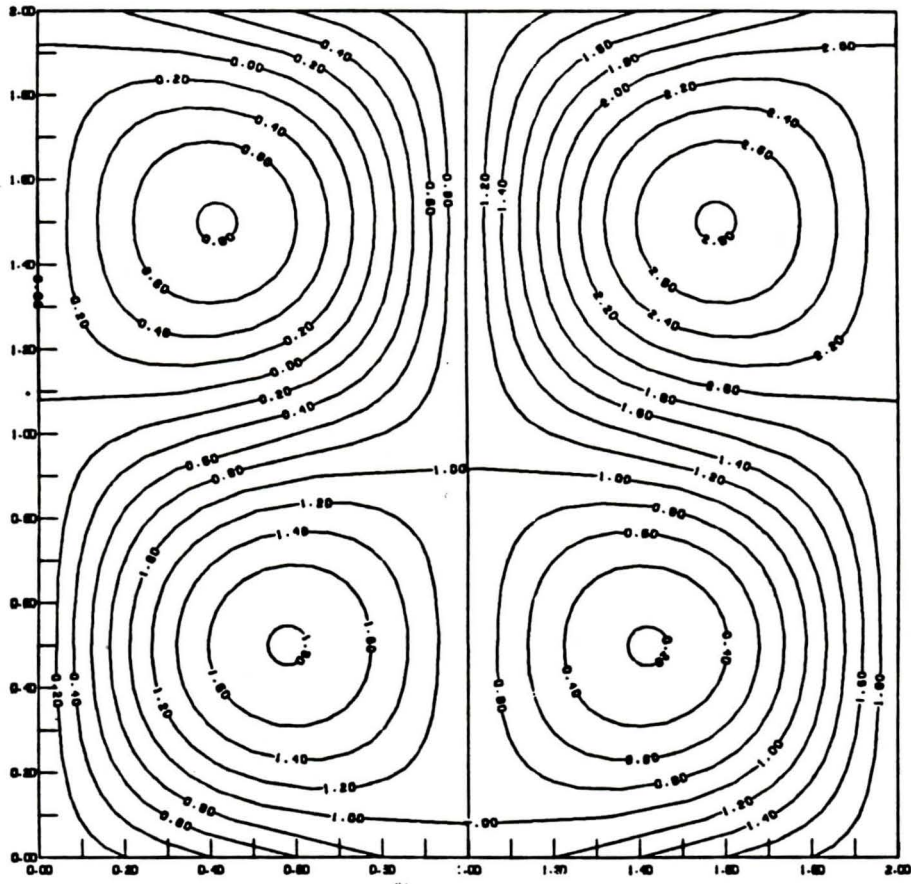


Figure 2

Particle streamlines for several values of s . Contours of v_x/v_s are plotted so that verticle cell boundaries are integer contours.

cell boundary. The large variations in yield distinguish tows which sample a region of retention from those which are taken in relatively plankton-free region between them. Tows perpendicular to the rolls sample both the plankton-dense and plankton-free regions.

For the remainder of this paper, we restrict the discussion to negatively buoyant particles in a cell in which the fluid motion is counter-clockwise. All results apply to positively buoyant particles and clockwise cells with the appropriate reversal of signs. Specifically, we will consider particles initially within the cell with fluid stagnation point at $(x = \frac{2\pi}{s}, y = \frac{2\pi}{s})$. This cell is the upper right quarter of figure 1. Let us denote the stagnation point of the particle motion by x_s . At this point the fluid velocity is directed upward and equal to the settling velocity of the particle in magnitude ($x_s = \sin^{-1}(s)$). For a given value of s , the orbit of a retained particle may be uniquely identified by the location of its right most crossing of a line of zero horizontal velocity ($y = n\pi, n = 0, 1, \dots$). The value of x at this point is denoted x_r . In steady flows, paths of particles with different initial positions do not cross unless they follow the same streamline.

The following observations of the motion of particles in steady flows were made with the numerical model described in section 4. Consider particles located within a region at retention. Figure 3 shows the period of the particle orbit as a function of x_r for several values of s . Near the fluid stagnation point, x_r , the fluid and $s = 0$ particles are in solid body rotation with period $P = 2\pi$. The period increases with increasing x_r , becoming infinite for a particle on an ascending cell boundary. For a given value of s , particles near the particle stagnation point have the minimum x_r and lowest period orbits. As s increases, the period of these tightest orbits ($x_r \sim x_s$) also increases. All particles with $x_r > x_s$ are retained.

The increase of the minimum period with s may be understood as follows. To simplify the algebra, shift the coordinate origin to the fluid stagnation point and let $A = 1$. The stream function is then

$$\psi_p(x,y) = \cos x \cos y + v_s x \quad (2.5)$$

Near the particle stagnation point ($x_s = \sin^{-1}(v)$, $y = 0$) the particle motion may be described by the first terms of a Taylor series

$$\begin{aligned} \dot{x}(x,y) &= \dot{x}(x_s, y_s) + (x-x_s) \left. \frac{\partial \dot{x}}{\partial x} \right|_{x_s, y_s} + (y-y_s) \left. \frac{\partial \dot{x}}{\partial y} \right|_{x_s, y_s} \\ \dot{y}(x,y) &= \dot{y}(x_s, y_s) + (x-x_s) \left. \frac{\partial \dot{y}}{\partial x} \right|_{x_s, y_s} + (y-y_s) \left. \frac{\partial \dot{y}}{\partial y} \right|_{x_s, y_s} \end{aligned} \quad (2.6)$$

or

$$\begin{aligned} \ddot{x} &= -\kappa y \\ \ddot{y} &= \kappa x \end{aligned} \quad (2.7)$$

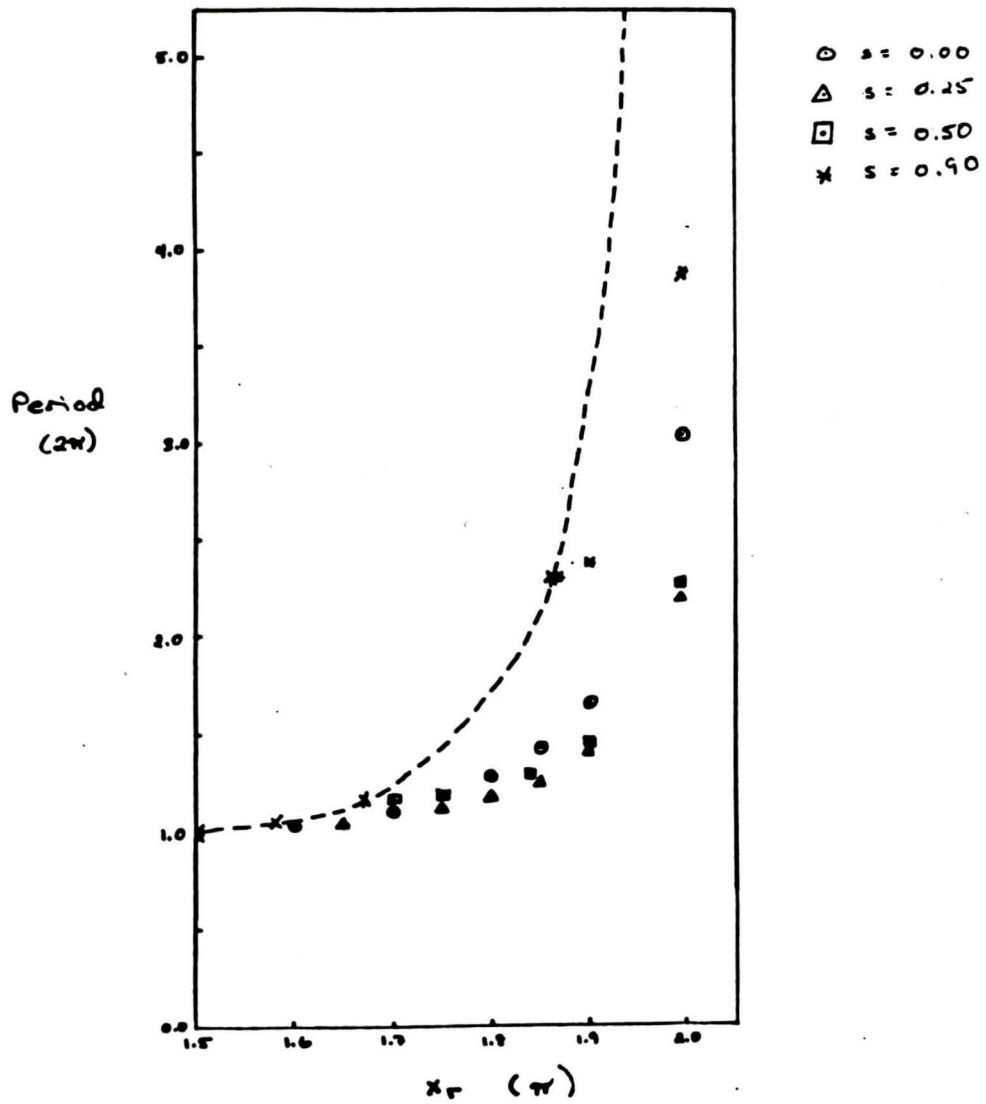


Figure 3. The period of retained particle orbits as a function of x for $s = 0.0, 0.25, 0.5$ and 0.9 .

where

$$\begin{aligned}
 X &= x - x_s \\
 Y &= y - y_s \\
 K &= \cos(x_s)
 \end{aligned}
 \tag{2.8}$$

Thus particles near the particle stagnation point are in solid body rotation with period

$$P = \frac{2\pi}{K}
 \tag{2.9}$$

This is the dashed line in figure 3. The cross marks along this line mark the location of the stagnation points for the numerical results shown in the figure.

3) PERIODIC BACKGROUND FLOW

To investigate the effects of allowing the background flow to vary in a periodic manner, redefine A as

$$A(t) = 1 + \epsilon \cos(\omega \alpha t) \quad (3.1)$$

where ϵ is the magnitude and ω the frequency of the oscillations of the fluid flow. The parameter α is used to separate time scales in the slowly varying case. With the coordinate origin at the fluid stagnation point, the stream function is now

$$\psi_p(x, y, t) = A(t) \cos x \cos y + v_s x \quad (3.2)$$

Two cases are considered analytically: first where the fluctuations about the mean flow are small ($\epsilon \ll 1$, $\alpha = 1$); and second, where oscillations in the flow occur on a time scale long relative to that of orbital periods ($\omega \alpha \ll 1$). In both cases, the expansions assume small x and y as measured from the relevant stagnation point.

Case A) Small Oscillations ($\epsilon \ll 1$)

Consider small oscillations about the mean flow ($\epsilon \ll 1$; $\alpha = 1$). Expanding the particle velocity field in x and y and retaining only linear terms yields

$$\begin{aligned} \dot{x} &= -A(t) y \\ \dot{y} &= A(t) x - v_s \end{aligned} \quad (3.3)$$

or

$$\begin{aligned} x_T &= -y \\ y_T &= x - v_s (1 - \epsilon \cos \omega T) + O(\epsilon^2) \end{aligned} \quad (3.4)$$

where a new time T has been defined such that

$$\begin{aligned} \frac{dT}{dt} &= \frac{1}{A(t)} \frac{dt}{dt} \\ T(t) &= t + \epsilon \left(\frac{1}{\omega} \sin \omega t \right) \end{aligned} \quad (3.5)$$

Note that $|T-t| \leq \frac{\epsilon}{\omega}$ for all t . Solving for $x(T)$, $y(T)$ yields

$$\begin{aligned} x(T) &= \alpha_0 \sin(T + \phi_0) + v_s - \epsilon \left(v_s \frac{\cos \omega T}{(1 - \omega^2)} \right) \\ y(T) &= -\alpha_0 \cos(T + \phi_0) - \epsilon \frac{v_s \omega}{(1 - \omega^2)} \sin \omega T \end{aligned} \quad (3.6)$$

where α_0 and ϕ_0 depend on the initial position of the particle. For $\omega = 0$ the motion is that of solid body rotation. For small ω , the particle makes order ϵ oscillations about the circular path centered on the particle stagnation point. This motion is observed in the numerical simulation. Figure 4a is a representative trace of particle motion.

Case B) Slow Oscillations ($\alpha \ll 1$)

In this case we reduce the third-order problem to one of elliptic integrals by suitable transformations. Specifically, we first transform from coordinates relative to the fluid stagnation point to an origin located on the particle stagnation point while rescaling time as in the small oscillation case. This transformation removes the constant terms in the velocity equations but introduces quadratic terms. These quadratic terms are then removed by an additional transformation so that the lowest order nonlinear terms are cubic. The resulting equations are solved for $(\dot{x})^2$ and the solution presented in terms of elliptic functions.

Recalling the initial equations

$$\begin{aligned} \dot{x} &= -A(t) \cos x \sin y \\ \dot{y} &= A(t) \sin x \cos y - v_s \\ A(t) &= 1 + \epsilon \cos(\omega \alpha t) \end{aligned} \tag{3.7}$$

first remove the constant term with the transformation

$$\begin{aligned} \xi &= x - x_0 \\ \eta &= y \\ \tau &= \alpha t \end{aligned} \tag{3.8}$$

where

$$\begin{aligned} v &= \frac{v_s}{A} \quad , \quad x_0 = \sin^{-1} v \\ \kappa &= \cos x_0 \end{aligned} \tag{3.9}$$

to obtain

$$\begin{aligned} \xi_\tau &= -\kappa \eta + v \xi \eta + \frac{\kappa}{2} \xi^2 \eta + \frac{\kappa}{6} \eta^3 \\ \eta_\tau &= \kappa \xi - \frac{v}{2} (\xi^2 + \eta^2) - \frac{\kappa}{6} \xi^3 - \frac{\kappa}{2} \xi \eta^2 \end{aligned} \tag{3.10}$$

which, upon rescaling, becomes

$$\begin{aligned} x_\tau &= -y + f(x, y) \\ y_\tau &= x + g(x, y) \end{aligned} \tag{3.11}$$

where

$$\begin{aligned} f(x, y) &= \frac{v}{\kappa} xy \\ g(x, y) &= -\frac{v}{2\kappa} (x^2 + y^2) \end{aligned} \tag{3.12}$$

The desired form is

$$\begin{aligned} \dot{\xi} &= -\eta + \mathcal{F}(\xi, \eta) \\ \dot{\eta} &= \xi + \mathcal{H}(\xi, \eta) \end{aligned} \tag{3.13}$$

where the lowest order terms in \mathcal{F} and \mathcal{H} are cubic. Define $\phi(\xi, \eta)$ and $\psi(\xi, \eta)$ such that

$$\begin{aligned} x &= \xi + \phi(\xi, \eta) \\ y &= \eta + \psi(\xi, \eta) \end{aligned} \tag{3.14}$$

From equations (3.11) and (3.14)

$$\begin{aligned} \frac{d}{dt} \begin{pmatrix} x \\ y \end{pmatrix} &= \begin{pmatrix} 0 & -1 \\ 1 & 0 \end{pmatrix} \begin{pmatrix} x \\ y \end{pmatrix} + \begin{pmatrix} f \\ g \end{pmatrix} \\ &= \begin{pmatrix} \dot{\xi} \\ \dot{\eta} \end{pmatrix} + \begin{pmatrix} \phi_{\xi} & \phi_{\eta} \\ \psi_{\xi} & \psi_{\eta} \end{pmatrix} \begin{pmatrix} \xi \\ \eta \end{pmatrix} \end{aligned} \tag{3.15}$$

$$\begin{pmatrix} 0 & -1 \\ 1 & 0 \end{pmatrix} \begin{pmatrix} \xi + \phi \\ \eta + \psi \end{pmatrix} + \begin{pmatrix} f \\ g \end{pmatrix} = \begin{pmatrix} \dot{\xi} \\ \dot{\eta} \end{pmatrix} + \begin{pmatrix} \phi_{\xi} & \phi_{\eta} \\ \psi_{\xi} & \psi_{\eta} \end{pmatrix} \begin{pmatrix} \xi \\ \eta \end{pmatrix} \tag{3.16}$$

and the requirement

$$\begin{pmatrix} \dot{\xi} \\ \dot{\eta} \end{pmatrix} = \begin{pmatrix} 0 & -1 \\ 1 & 0 \end{pmatrix} \begin{pmatrix} \xi \\ \eta \end{pmatrix} + \begin{pmatrix} \mathcal{F} \\ \mathcal{H} \end{pmatrix} \tag{3.17}$$

Expansion of $\phi(\xi, \eta)$ and $\psi(\xi, \eta)$ in Taylor series

$$\begin{aligned} \phi(\xi, \eta) &= A_1 \xi^2 + B_1 \xi \eta + C_1 \eta^2 + \phi_3(\xi, \eta) + \dots \\ &= \phi_2(\xi, \eta) + \phi_3(\xi, \eta) + \dots \\ \psi(\xi, \eta) &= \psi_2(\xi, \eta) + \psi_3(\xi, \eta) + \dots \end{aligned} \tag{3.18}$$

and substitution into equation (3.15) yields, for ϕ_2 and ψ_2

$$\begin{aligned} -\eta \phi_{\xi} + \xi \phi_{\eta} + \psi - f &= 0 \\ -\eta \psi_{\xi} + \xi \psi_{\eta} - \phi - g &= 0 \end{aligned} \tag{3.19}$$

Determining the quadratic parts of $f(x,y)$ and $g(x,y)$ in terms of ξ and η and solving the above equations for ϕ_2 and ψ_2 yields

$$\begin{aligned}\phi_2(\xi, \eta) &= \frac{v}{6} \xi^2 + \frac{5v}{6} \eta^2 \\ \psi_2(\xi, \eta) &= -\frac{2v}{6} \xi \eta\end{aligned}\quad (3.20)$$

With equation (3.20) and the rescaling

$$x = \beta \xi \quad y = \beta \eta \quad \beta = \left(\frac{v}{\gamma}\right)^{1/2} \quad (3.21)$$

equations (3.17) become

$$\begin{aligned}\dot{x} &= -y - x^2y + 5y^3 \\ \dot{y} &= x - 3xy^2 - x^3\end{aligned}\quad (3.22)$$

Eliminating y yields

$$\ddot{x} = -x + 10x(\dot{x})^2 \quad (3.23)$$

or

$$(\dot{x})^2 = A e^{10x^2} + \frac{1}{10} \quad (3.24)$$

Expanding the exponential and solving the truncated system as an elliptic integral yields (Abramowitz and Stegun (1964))

$$x = \frac{b}{\sqrt{a}} \operatorname{sc}(t, \frac{a^2 - b^2}{a^2}) \quad (3.25)$$

where

$$\begin{aligned}a^2 &= \frac{1}{10} \left(1 + \left(-\left(1 + \frac{1}{\sqrt{10}} \right) \right)^{1/2} \right) \\ b^2 &= \frac{1}{10} \left(1 - \left(-\left(1 + \frac{1}{\sqrt{10}} \right) \right)^{1/2} \right)\end{aligned}\quad (3.26)$$

and sc is a Jacobian elliptic function. The process must now be repeated allowing the constants of this case to become functions of the slow time, τ .

4) NUMERICAL EXPERIMENTS

In order to explore particle motion outside those areas accessible to analytic investigation, a numerical model of the tank was constructed. The model evolves the particle position given the fluid flow field of equation (2.1) with $A(t)$ as in equation (3.1). We simulate the region $0 \leq x \leq 2$; $0 \leq y \leq 2$ with periodic boundary conditions. Any particle passing through the bottom $(x,0)$ is reintroduced at the top $(x, 2\pi)$. A particle which passes through the bottom boundary is said to "fall out" of the cell, as opposed to a "retained" particle which does not cross a horizontal cell boundary. The horizontal motion of the particles is strictly that of the fluid, thus contours of zero horizontal fluid velocity, such as the lines

$y = n\pi$, $n = 0, 1, 2, \dots$, are barriers which the particles cannot cross. None were observed to do so. As noted above, all particles were initially placed in the counter-clockwise cell which is centered at $(1.5\pi, 1.5\pi)$.

Observations with a steady fluid flow were noted in Section 2 above. When the flow becomes periodic, there is a qualitative change in the regions of retention. In the steady case, negatively buoyant particles arbitrarily near an upflowing branch are retained, completing closed orbits. This is apparent in the lower part of figure 2a where the retention regions of two horizontally adjacent cells appear to merge across the cell boundary. In periodic flow, each region of retention is separated from the cell boundary by a finite band. Particles initially in this band will often remain in the cell for many revolutions, but will fall out. The physical explanation of the phenomenon is straightforward. For small ϵ , a particle oscillates about its equilibrium path. As long as these excursions are completely within the region of retention, the particle will remain in the cell. A particle which oscillates to a point outside the retention region may remain in the cell for a time, depending on where in the cell it is when it crosses the boundary. Eventually, most such particles will cross the boundary near the bottom of their trajectories and fall out of the cell. It is conceivable that, for certain initial positions, a resonance between the fluid oscillations and the particle orbital motions occurs which tends to stabilize the particle. While the stabilization of particles in regions which are unstable in the mean flow has not been observed, some particles tracing orbits which do not lie entirely within the retention region for the steady flow corresponding to $A = (1 - \epsilon)$, are retained for the entire observation period (1000 fluid periods) and appear stable.

Consider the paths of particles near the region of retention which, after some time in the initial cell, fall out. When these paths are strobed, chaotic motion is observed. A particle well within the region of retention will remain in the cell for the entire observation period (over 5000 fluid periods), while a particle far outside the region will fall through the cell with an average residence time of approximately one period. A particle in this intermediate region falls out of the original cell, usually passing quickly through several cells before being reentrained. The residence time averaged over a chaotic fall through 500 cells is typically 15 periods per cell. Figure 9 is a histogram of the frequency of various residence times. It is clear that these particles take much longer to fall through a series of rolls than would be predicted from the steady case.

Examples of these motions are shown in figure 10. Particles well within the region of retention display two distinct classes of motion. In the first, a generalization of oscillations about the mean path, the particle moves within the bounds of the two orbits for the steady flow with $A = (1 + \epsilon)$ and $A = (1 - \epsilon)$. The particle track fills in a two-dimensional cross-section of a donut, oscillating back and forth along a path which does not close on itself (figures 4 and 5). When the position of the particle is recorded once per cycle of the background fluid flow, the resulting graph is a cross-section (an x, y plot at given phase) of the three-dimensional phase space of the system. Figure 4b is the motion of the particle shown in figure 4a strobed in this way. By strobing at different phases it is seen that the particle winds about on a torus in phase space. Since a single point in phase space defines the future evolution of the system, the particles located within closed curves on Poincare sections are trapped there.

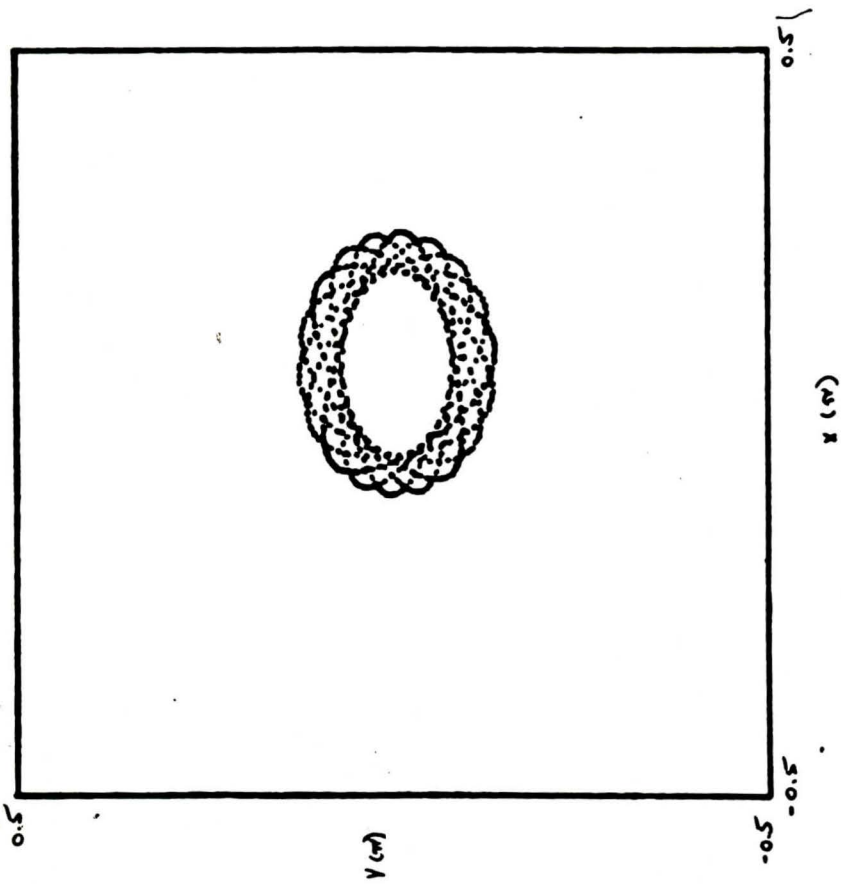
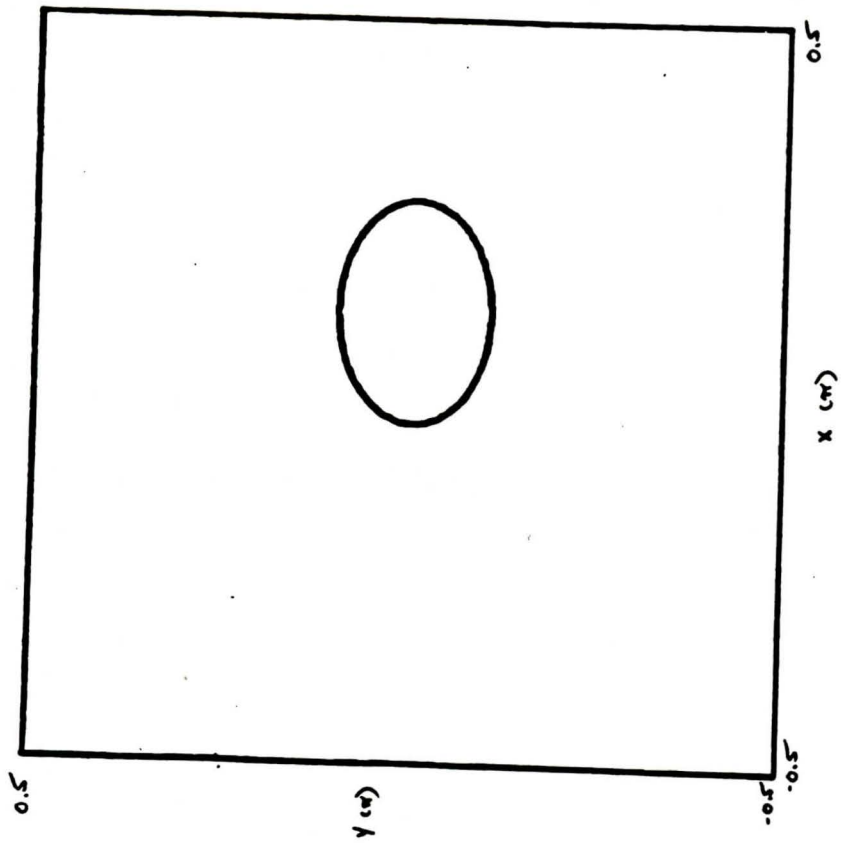


Figure 4

Solution for small amplitude oscillations. Here $X_0 = 0.10$;
 $Y_0 = 0.10$ (see equation 3.2); $V_s = 0.25$; $\epsilon = 0.5$; $P = 4.0$;
(A) Particle track with $T_{max} = 100$.
(B) Strobbed particle motion with $T_{max} = 4000$.

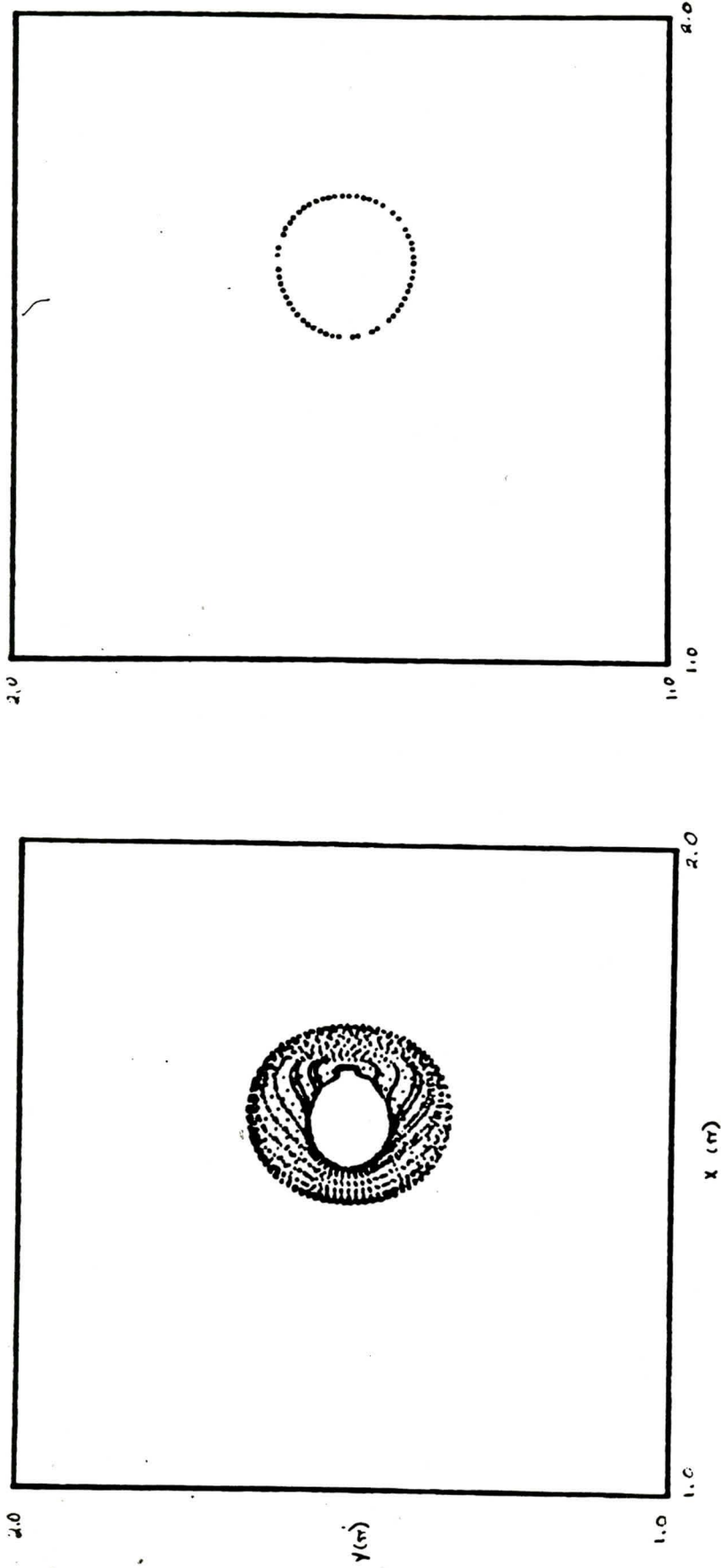


Figure 5

Model particle trajectory with $X_0 = 1.50$; $Y_0 = 1.50$;
 $V_s = 0.25$; $\mathcal{E} = 0.50$; $P = 4.40$. (A) Particle
track with $T_{max} = 250$. (B) Strobed particle motion
with $T_{max} = 2500$.

A second behavior is observed when the particle completes an integral number of revolutions about the stagnation point in an integral number of fluid oscillations. During each revolution about x_g , the particle follows one of several distinct pathways. Which path is executed depends on the phase of the flow as the particle crosses the x axis from below ($x > x_g$). An example of this type of motion is shown in figure 6. The clear regions shown remain clear, with the particle being restricted to and slowly filling the outlined region. In this example two revolutions about the stagnation point, one along each branch, occur in three cycles of the background fluid flow. We shall call this completion of the motion (several revolutions until the crossing of the x axis occurs at approximately the same position and phase) a particle orbit. In this case the particle orbital period is three times the fluid flow period.

When this motion is strobed at the fluid flow frequency, islands are observed (figure 7). Particle motion on these islands is stable for all times observed. The particle visits every island in turn, slowly delineating each. Poincare sections taken at different phases are shown in figure 8. The islands slowly deform and rotate in the direction of particle motion until, one full fluid period later, particles initially on island 1 (2,3) have taken positions on island 3 (1,2). Recalling that these figures are cross-sections of a three-dimensional phase space, it is seen that this motion takes place on a torus which is stretched and twisted, closing on itself in three fluid periods. Particle paths wind around on this torus.

Particles initially just inside or outside the island ring (relative to the particle stagnation point) wind about a single torus. Particles within the boundaries of an island wind about a similarly twisted torus always bounded by the outer torus (coaxially). Particles initially located between the islands at the same distance from the stagnation point are observed to display chaotic motion contained by the tori which bound the island ring.

The strobed paths for a variety of initial positions are shown in figure 10. Counting from the left, the first particle (1.1π , 1.5π) falls through the cell, oscillating about the strobed path shown. This line presents a barrier which other particles do not cross - hence the open region in the lower left-hand side of the figure. This open area is occupied by the mirror particles of those plotted. As the initial position of the point is moved to the right along $y = 1.5 \pi$, this curve breaks up into islands, which in turn becomes part of the chaotic sea shown in the figure. Particles initially in this area are found to become trapped in a cell for many revolutions and then fall (drifting) through the cell (often several) before becoming reentrained. Embedded in this chaotic sea are regions avoided by the falling particle. The largest of such areas is the region of retention containing the particle stagnation point. Islands are observed in this and several other of the barren regions where the particle motion is such that they are stabilized against fall out by the oscillations. An example of this behavior is the particle whose motion produces the "ears" in figure 10. Here the period of the particle motion is such that the maximum of the fluid flow occurs twice in each revolution - once at the top of the trajectory and once at the bottom. Particles following these trajectories travel outside the region of retention for a steady flow with $A = (1-\epsilon)$. The three islands located within the retention region ("eyes" and "mouth") are the same islands shown in figure 7. Also shown are one enclosed and one encompassing torus.

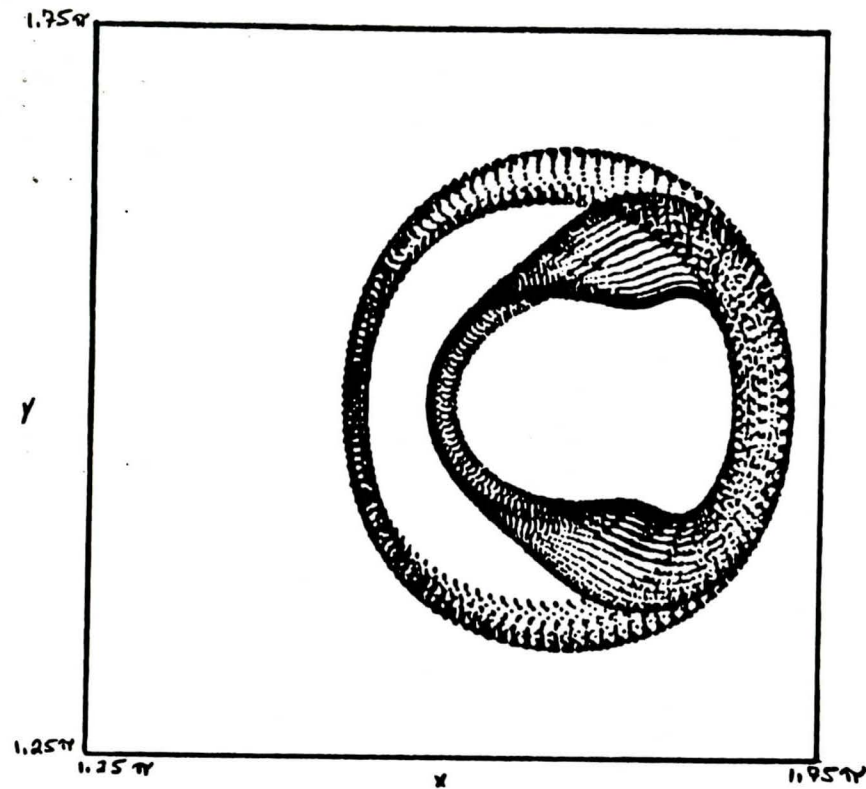


Figure 6

Particle trajectory characteristic of islands. In this case $X_0 = 1.50$; $Y_0 = 1.50$; $V = 0.25$; $\epsilon = 0.50$; $P = 4.50$. Note that this figure is an enlargement of the cell.

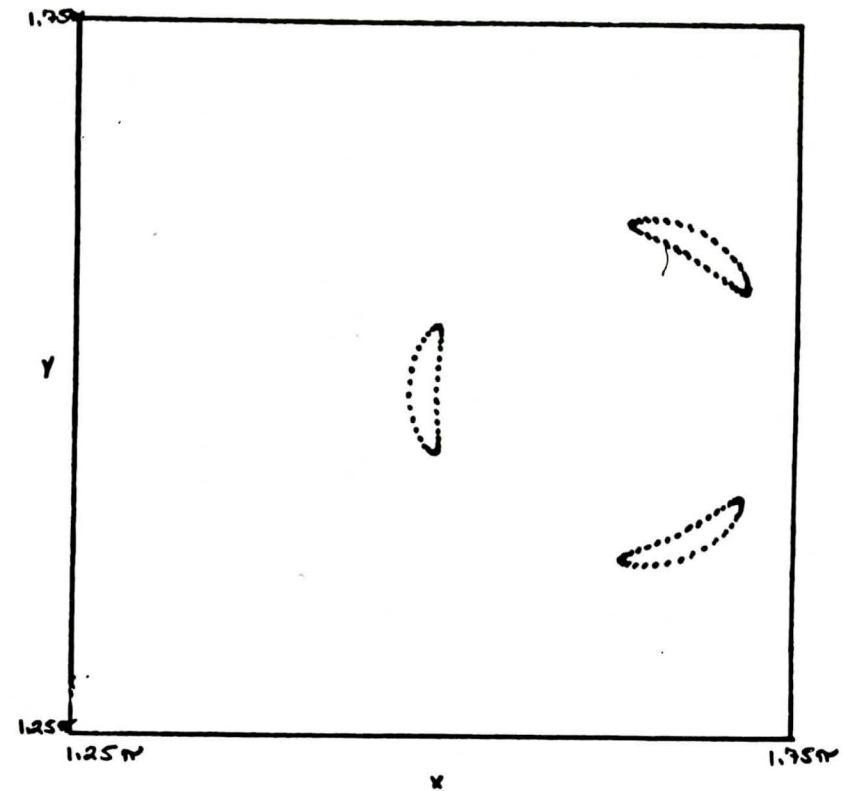


Figure 7

Particle path of figure 6 stopped at the frequency of the fluid oscillations. $T_{max} = 1000$.

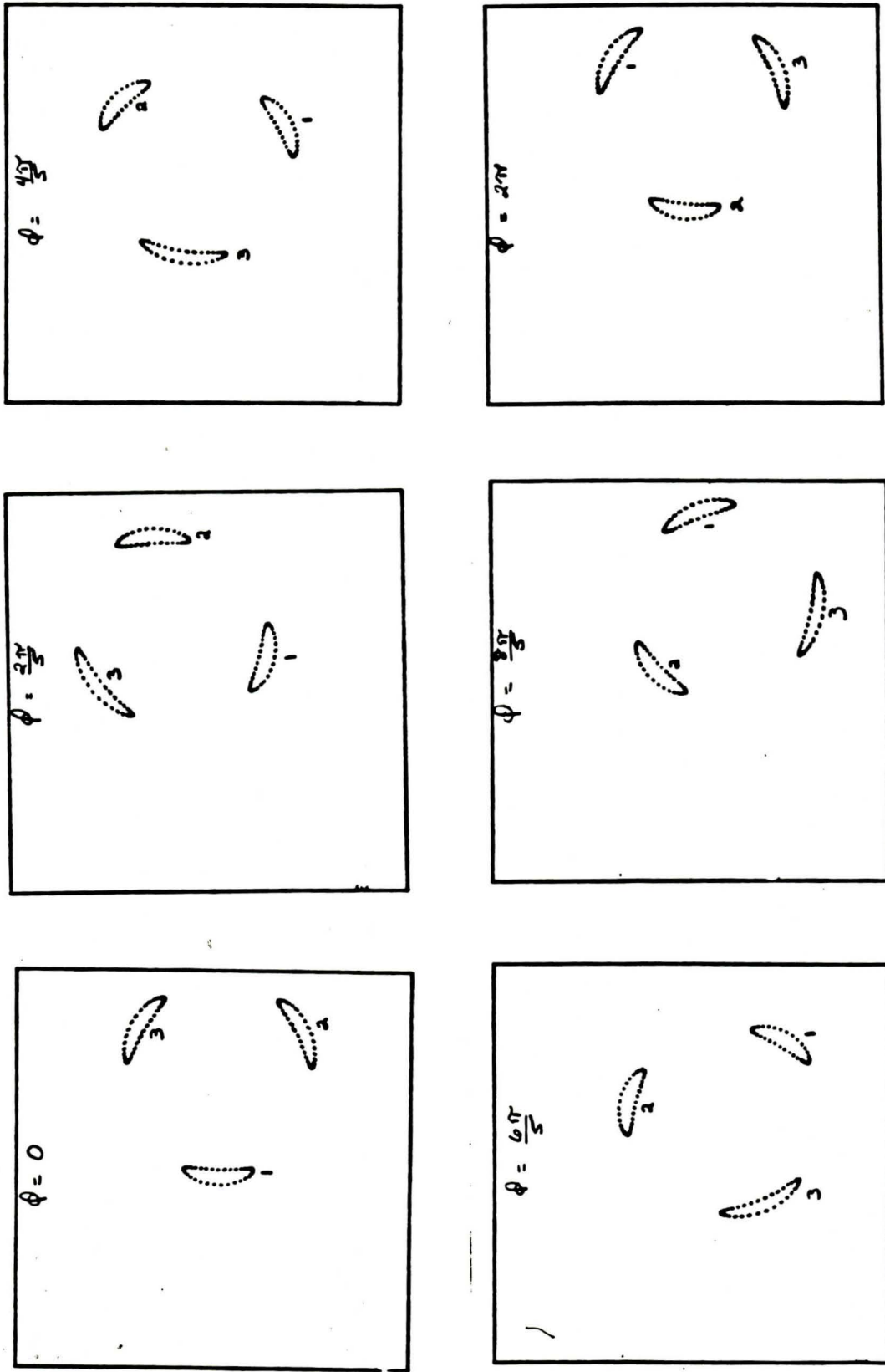


Figure 8

Location of the islands of figure 7 at various phases of the fluid flow. The region shown in each box above is the same as shown in figure 6.

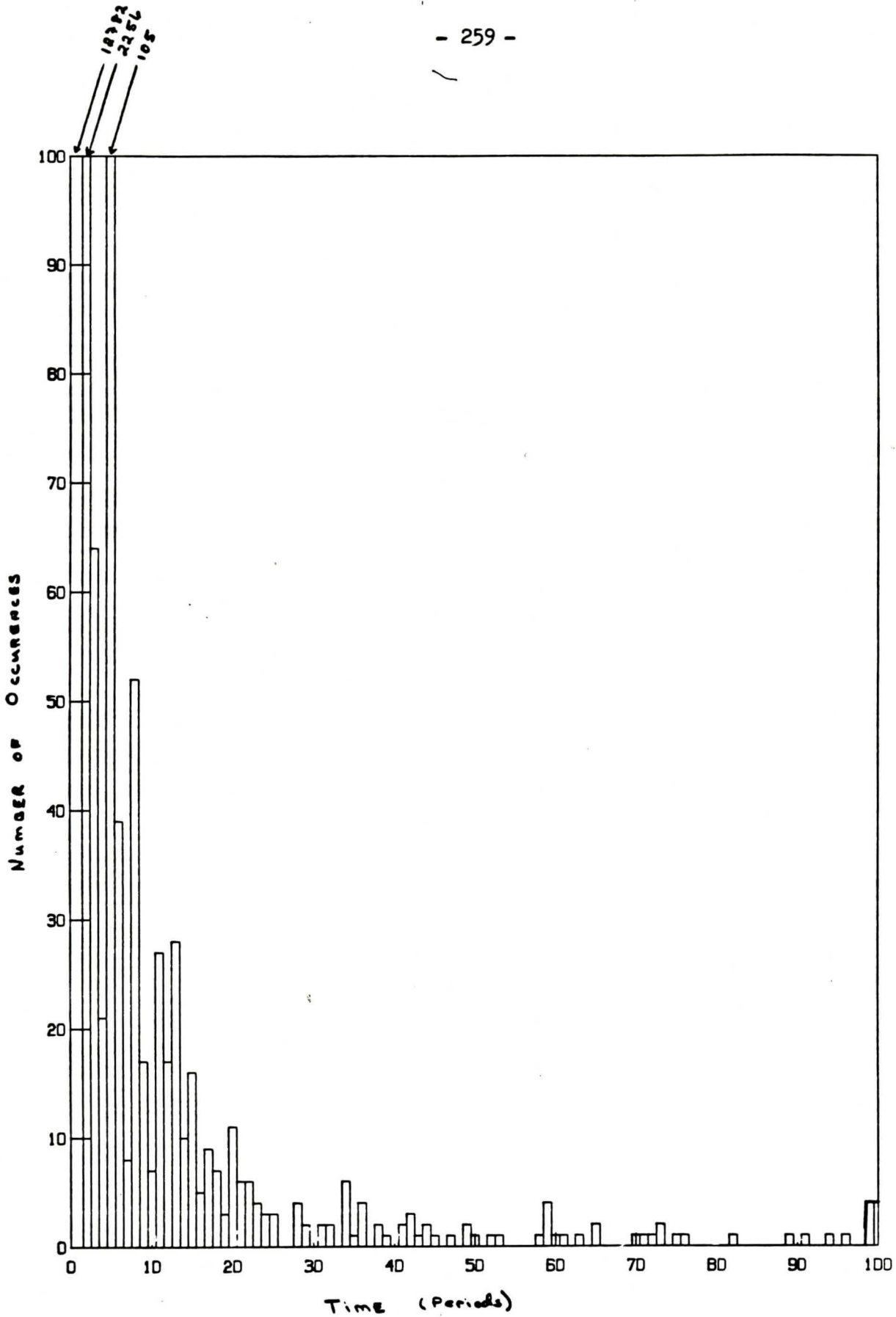


Figure 9

A sample histogram showing the relative frequency of various residence times for particles in the fallout region. Maximum time observed = 100 periods.
 $V_s = 0.25$; $\epsilon = 0.50$; $P = 4.50$.

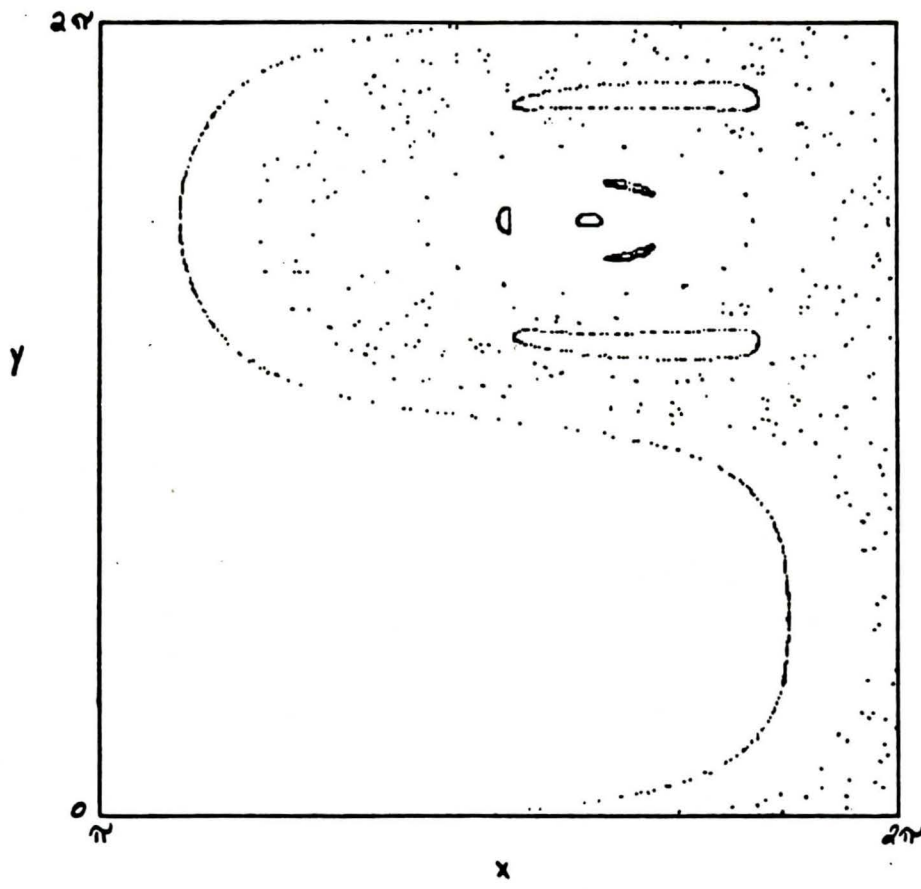


Figure 10

Strobed motions of six particles with $V_s = 0.25$;
 $\epsilon = 0.50$; $P = 4.50$.

Whether particles outside the mean region of retention can be stabilized by the fluid oscillations is a question which deserves further investigation. Here we briefly note some initial observations with regard to the effect of increasing the magnitude of the flow oscillations on the retention of particles in marginally stable regions. Figure 11 shows the region of the upper ear in figure 10 for several values of ϵ . At small ϵ , a stable orbit is observed. As ϵ increases this torus breaks up into islands and then disintegrates altogether, the particles falling through the cell after only a few revolutions. As ϵ is increased further, the region again begins to stabilize - particles still fall through, however they spend a great deal of time in these quasi-stable regions between vertical drops.

At very large values of ϵ a different type of behavior is observed. Figure 12 displays the strobed trajectories for particles with the same initial positions as those in figure 10, with $\epsilon = 8.0$. For $\epsilon > 1$, the flow reverses direction. Quasistable particle motion is observed to be centered about the stagnation point of the fluid. A large portion of the cell is subject to chaotic particle motions. The three island ring and fuzzy inner and outer elliptical paths are observed to be slowly evolving outward. The evolution of the islands is much slower than that of either of the simple tori. It would be interesting to observe how (if) the particles within the island ring escape. Although their orbits are evolving outward, the inner particles in figure 10 are still in the initial cell after over 500 periods of the fluid flow.

The motion at large ϵ is qualitatively different from that of small ϵ (see figure 13). Quasistable regions in this flow have been found where the particle revolution period is slightly less than half the fluid period. Such a particle, initially near the top of its orbit will be swept around by the strong flow, again to near the top of the cell, as the flow weakens it will sink down toward the cell center and then be swept around in the opposite direction sense by the second half cycle of the fluid flow. Often the radius of the particle from the stagnation point will increase until the particle falls out, however some initial conditions particles have been observed to be carried up above their initial points and then dropped back near their original position (and phase). In this manner the particle is retained in the cell for a very long time ($t \gg t_{\text{max observations}} = 500$ fluid periods).

5) CONCLUDING REMARKS

The motion of slowly sinking particles in a simple time dependent flow has been examined. It is found that this system is quite rich, displaying a surprising variety of particle motions. In addition to bounded chaotic motions, particles falling through the cells chaotically are often entrained and retained for significant periods of time, so that the sedimentation rate in this case varies substantially from the case of steady rolls. Investigations of the effects of both small and large fluid oscillations reveal that retained particles are more stable than might be expected.

The model may be extended to consider inertial effects. These will not necessarily be destabilizing, especially in the case of large fluid oscillations. Inclusion of Brownian motion would allow migration across vertical cell boundaries, as well as into and out of regions of retention, with interesting effects on the mean sedimentation rate. More applied problems,

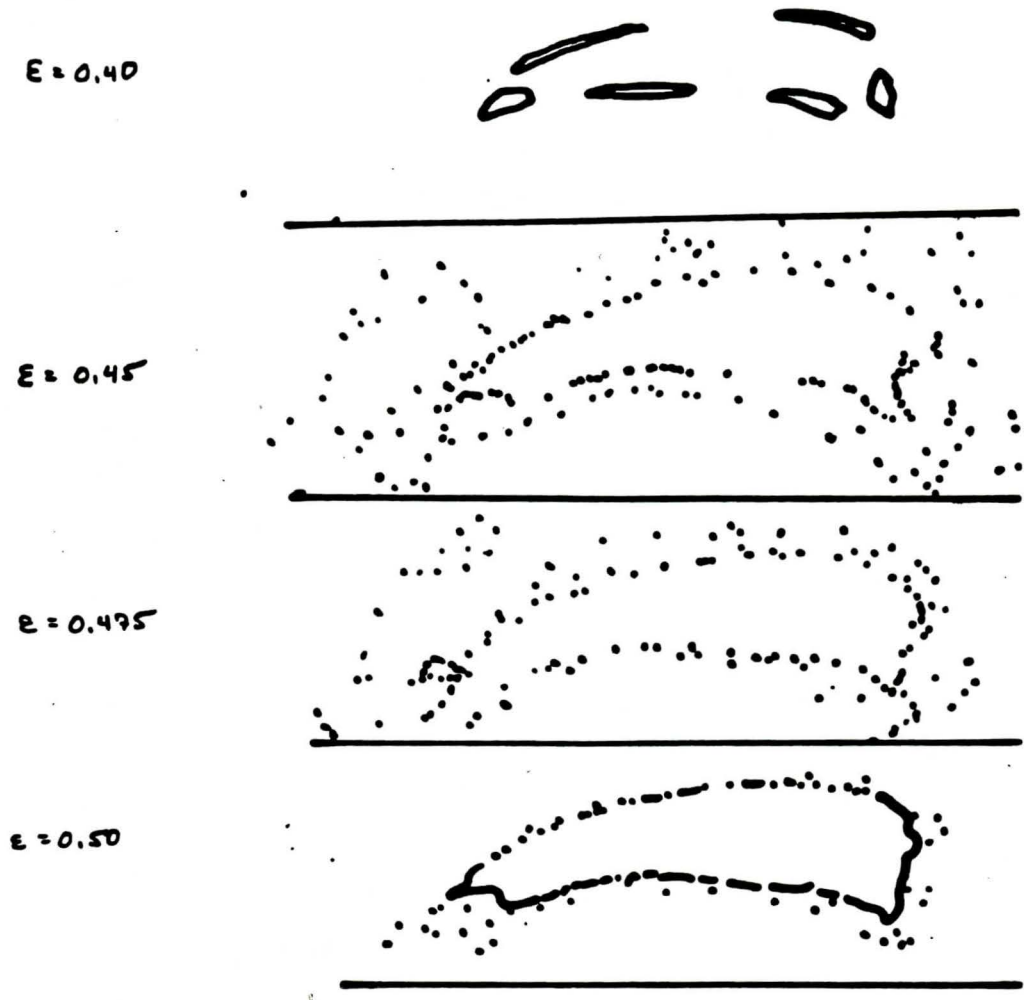


Figure 11

Relative stability of the ear region of figure 10 for several values of ϵ .

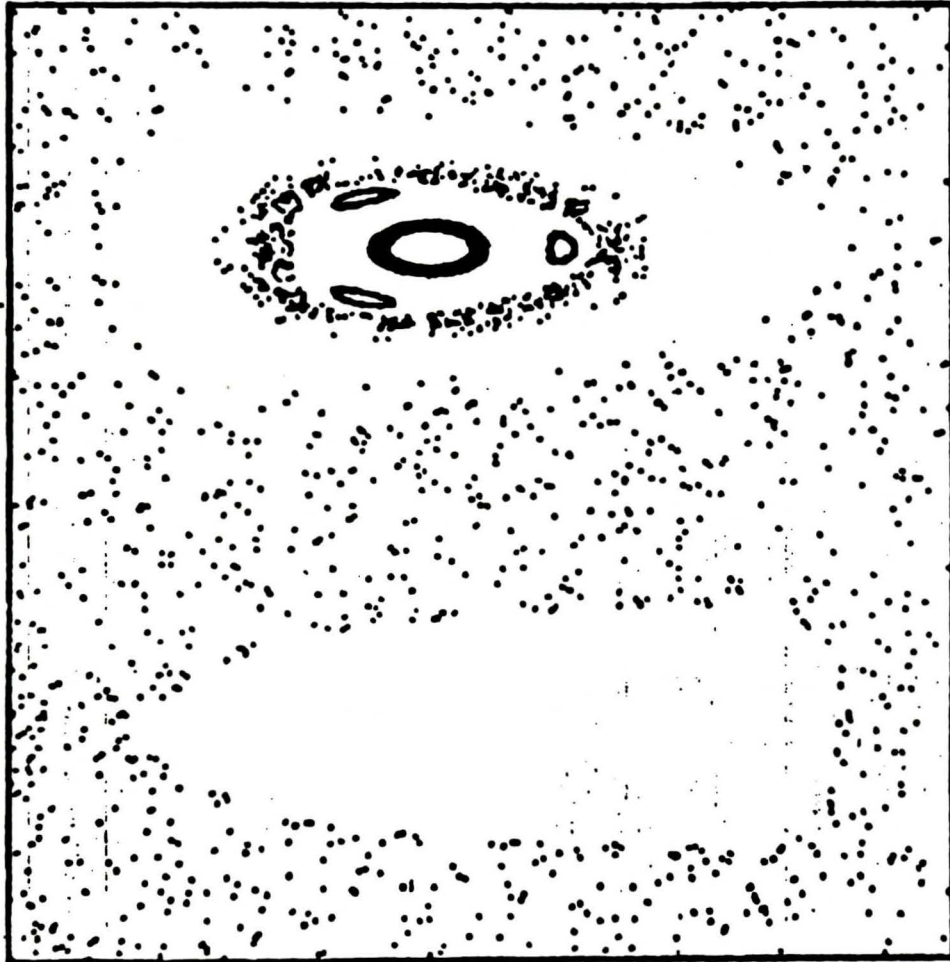


Figure 12

Strobed motions of six particles with $V_S = 0.25$;
 $\epsilon = 0.50$; $P = 8.00$.

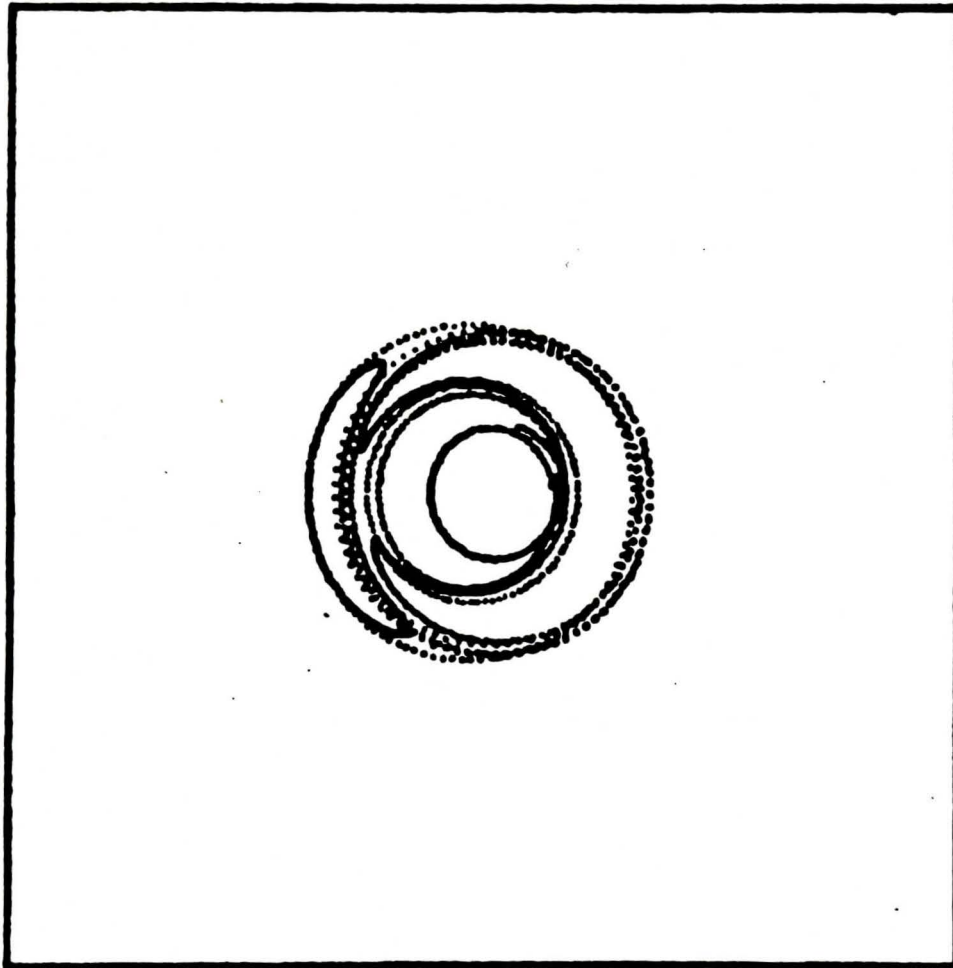


Figure 13

Particle track with $\epsilon = 8.0$; $V_s = 0.25$; $P = 4.50$.

such as precipitation and magma crystal growth may be approached by including a growth parameter which is a function of location and time. In all, this type of model provides a foothold into many topics of current interest.

ACKNOWLEDGEMENTS

I would like to express my thanks to Dr. E. A. Spiegel for his guidance and enthusiasm with this problem to the Staff and Fellows of the Summer Program for their discussions and fellowship, and to Dr. H. Huppert for introducing the problem to us. The suggestions and observations of C. N. Corfield and Dr. M.P.E. Proctor regarding the analytic portions are gratefully acknowledged. I thank Dr. J. Whitehead for making his experimental apparatus available to me and R. Frazel for technical assistance.

REFERENCES

- Abramowitz, M. and L. Stegun, 1964. Handbook of Mathematical Functions. U. S. Government Printing Office, Washington, D. C.
- Aref, H., 1984. Stirring by chaotic advection. J. Fluid Mech., 143, 1.
- Stommel, H., 1949. Trajectories of small bodies sinking slowly through convection cells. J. Mar. Res., 8, 24.
- Tooby, P., G. Wick and J. Isaacs, 1977. The motion of a small sphere in a rotating velocity field. J. Geophys. Res., 82, 2096.